

# Properties of nano-composite SACX0307-(ZnO, TiO<sub>2</sub>) solders

Balázs Illés\*, Agata Skwarek<sup>††</sup>, Oliver Krammer\*, Tamás Hurtony\*, Dániel Straubinger\*, Jacek Ratajczak<sup>§</sup>, Gábor Harsányi\*, and Krzysztof Witek<sup>†</sup>

\* Budapest University of Technology and Economics, Faculty of Electrical Engineering and Informatics, Department of Electronics Technology, Budapest, Hungary  
Email: billes@ett.bme.hu

<sup>†</sup>Łukasiewicz Research Network - Institute of Microelectronics and Photonics, LTCC Technology and Printed Electronics Research Group, Kraków, Poland  
Email: agata.skwarek@imif.lukasiewicz.gov.pl

<sup>‡</sup> Gdynia Maritime University, Department of Marine Electronics, Gdynia, Poland

<sup>§</sup>Łukasiewicz Research Network - Characterization of Materials and Instruments Research Group, Warsaw, Poland  
Email:jacek.ratajczak@imif.lukasiewicz.gov.pl

**Abstract**— In the present study, SACX0307-ZnO and SACX0307-TiO<sub>2</sub> nano-composite solder pastes were fabricated. The ceramic reinforcements were used in 1wt% and with different primary particle sizes between 50-200nm. The soldering properties and microstructure of the solder joints were investigated. The nano-particles were mixed into the solder paste by standard ball milling process. Reflow soldering technology has been applied to prepare solder joints and spreading tests from the different solder alloys. The solder joints were evaluated by shear test, and cross-sections were prepared to investigate the metallographic properties by Scanning Electron Microscopy (SEM). The different ceramic nano-particles had different effects on the solderability of solder alloys. Best results were observed in the case of TiO<sub>2</sub> nano-particles with improved wetting and mechanical strength. The microstructural investigations showed considerable grain refinement and the modified grain boundary/interfacial properties, which could cause the increase of the mechanical parameters.

**Keywords**—soldering; nano-composite; SACX; grain refinement; ZnO; TiO<sub>2</sub>.

## I. INTRODUCTION

The ban of the lead content solder alloys in the electronics industry resulted in the use of the 96.5Sn3Ag0.5Cu (called SAC305) and 95.5Sn4Ag0.5Cu (called SAC405) solder alloys [1]. Both of them are having relatively high Ag content, which increased their price (compared to the SnPb solder alloys), and it could arise potential reliability issues such as shrinkage defects. It can occur when the Ag<sub>3</sub>Sn intermetallic compounds (IMCs) form islands during the solidification of the solder alloy [2]. So in the past decade, strong researches were carried out in order to be able to reduce the Ag content in the SAC solder alloys. The most known low-silver content candidate is the 99Sn0.3Ag0.7Cu (called SAC0307) solder alloy. It usually contains some further metals (like Co, Sb, Bi, Ni, etc.) in very low amounts (under 0.1 wt%), so it is called as well to “micro-alloyed” solder. In this case, the abbreviation is SACX0307. These further metals improve the mechanical and wetting properties of the alloy, which could be decreased due to the lower Ag content.

The latest method to improve the quality and reliability of the lead-free solder alloys is the use of ceramic reinforcement particles in the solder paste and create a so-called “composite solder alloy”. A wide range of ceramics, like TiO<sub>2</sub>, ZrO<sub>2</sub>, Al<sub>2</sub>O<sub>3</sub>, Fe<sub>2</sub>O<sub>3</sub>, Si<sub>3</sub>Ni<sub>4</sub>, SiC, La<sub>2</sub>O<sub>3</sub>, were already used mostly in SAC015, SAC305, SAC405 alloys [3]. The size of the ceramic particles is in the submicron and mostly in the nano range, and they are used in the amount of 0.05 wt% to 2 wt%. The reinforcement particles have a strong effect, mostly on the grain growth during the solidification process, so they can result in a totally different microstructure ( $\beta$ -Sn grain size and IMC structure) [3]. The most applied ceramics are the TiO<sub>2</sub> and the ZnO due to their relatively low prices and easy availability.

It was reported that TiO<sub>2</sub> could suppress the IMC layer growth [4-5]. However, Shengyan et al. found that TiO<sub>2</sub> nano-particles can create a considerable stress concentration among the IMCs, which can cause the breakage of Cu<sub>6</sub>Sn<sub>5</sub> IMCs during its growth phase and finally causes a potential reliability issue [4]. Moreover the addition of TiO<sub>2</sub> nano-particles could also decrease the Ag<sub>3</sub>Sn grain size and the interphase spacing between them, which resulted in further microhardness enhancement [6]. An unfavorable side effect of the TiO<sub>2</sub> addition can be the increase of the melting point of the composite solder alloy [7]; however, it is usually only some Kelvin [8]. Furthermore, the ceramic particles can marginally increase the resistance of the solder joints.

The addition of ZnO particles has a similar effects. Qu et al. showed that the ZnO micro- and nano-particles in SAC305 solder alloy decreased the IMC layer thickness at the solder-substrate interface [9]. They observed some wettability increase over 0.5 wt% as well [10]. Qu et al. have also proved that ZnO nano-particles can decrease the diffusion trough the IMC layer and slow down the constant and enhanced IMC formation during high temperature aging test [11]. This can be considered as a positive reliability effect of the ZnO ceramics. Al-Ganainy et al. found better creep life and creep resistance after the addition ZnO ceramic particles into

93.5Sn6.5Zn solder alloy [12]. Some Kelvin of melting temperature increase of the SAC alloys can also be occurred after the application of ZnO, as was reported by El-Rehim et al. after differential scanning calorimetry measurements [13]. The reinforcements can modify the viscosity parameters and, with this, the printability of the solder paste. Kanlayasiri et al. found that the addition up to 1 wt% ZnO nano-particles into SAC0307 solder paste decreased the cold slump properties [14]. Printability problems have also been found by Kanlayasiri et al. in the case of higher ZnO nano-particles concentration [15].

Most of the previous studies have investigated only bulk solder materials. The properties of the composite solder alloys can differ in the case of real assemblies, in the case of the presence of soldered components [16]. Therefore our aim was to investigate the soldering properties of nano-composite SACX0307-ZnO and SACX037-TiO<sub>2</sub> solder alloys in their real “environment” as real solder joints.

## II. MATERIALS AND METHODS

Nano-composite solder alloys have been made from SACX0307 (Alpha SACX 0307 CVP 390 PBF) and from TiO<sub>2</sub> and ZnO nano-particles. The primary particle sizes of the TiO<sub>2</sub> nano-particles were 100 nm (Sigma-Aldrich 634662-25G) and 200 nm (Sigma-Aldrich 232033-500G), respectively. The primary particle sizes of the Zn nano-particles were 50 nm (Sigma-Aldrich 677450-5G), 100 nm (Sigma-Aldrich 544906-10G-5G), and 200 nm (Sigma-Aldrich 96479-100G), respectively. The nano-particles were applied in 1wt%, and they were mixed into the solder paste homogeneously using the ball milling process. The mixing was carried out by a planetary ball miller at 300 rpm for 10 mins. The studied nano-composite solder alloys can be seen in Table 1.

**Table 1.** Investigated solder alloys.

Sample name	Composition
REF	SACX0307
T1	SACX0307-TiO <sub>2</sub> (200 nm)
T2	SACX0307-TiO <sub>2</sub> (100 nm)
Z1	SACX0307-ZnO (200 nm)
Z2	SACX0307-ZnO (100 nm)
Z3	SACX0307-ZnO (50nm)

In the first step, spreading tests were done to study the wettability of the different solder pastes. The test surfaces were prepared on FR4 substrate from laminated Cu layer (in 50x50mm dimensions) with Ag surface finishing. The printed deposits had 5mm diameter. Four round-shaped solder drops were screen-printed onto the test surface. The printed solder drops have been reflowed by IR batch oven. The wetted area was investigated and measured by an Olympus BX50 optical microscope. The spreading tests were repeated 16 times in the case of each sample type.

In the second step, solder joints were prepared from 0603 chip resistors on daisy-chain type FR4 test boards (Fig. 1). The preparation has followed the steps of the classical SMT: solder paste was screen-printed onto the contact pads with a 125 μm thick stencil; the chip resistors were placed onto the solder deposits; and finally, the assembly was soldered in an IR batch reflow oven under air atmosphere. The soldering was done with a linear thermal profile: 180–190 °C pre-heating for 180s, 245–255 °C ramp-up for 60s, and 150 °C cool down for 100s.

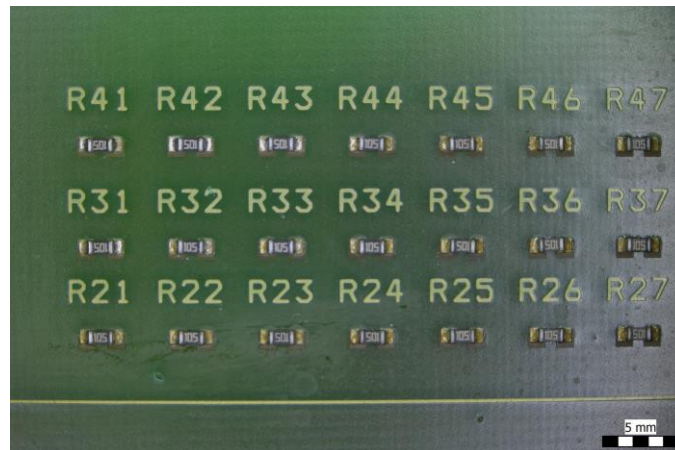


**Fig. 1.** Solder joints on the FR4 test board.

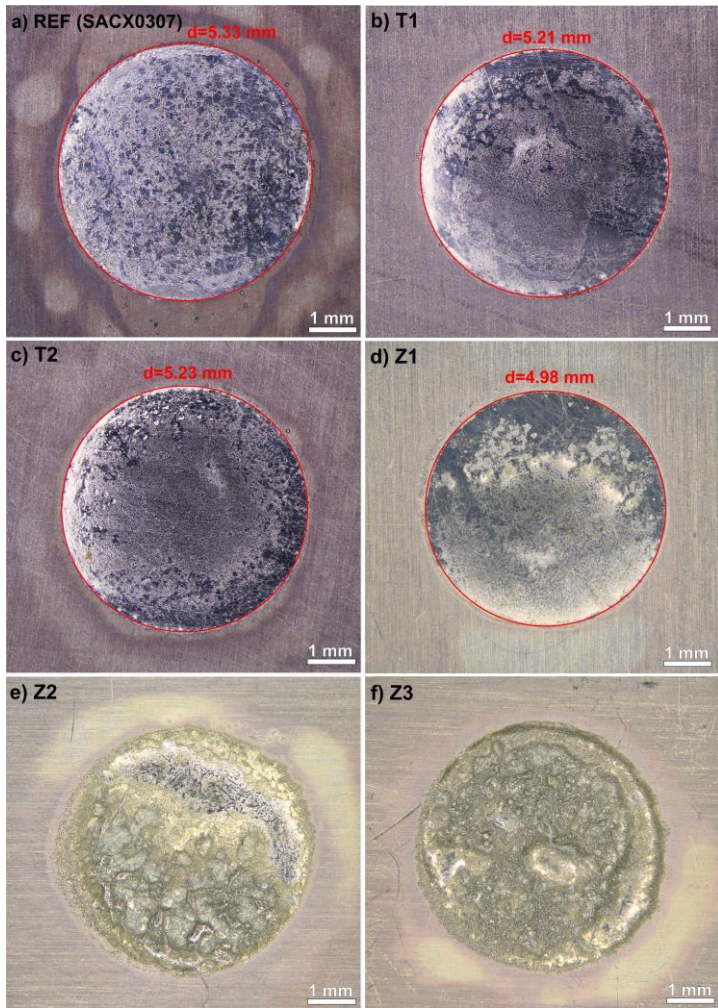
The solder joints were evaluated by shear strength measurements using a DAGE 2400 shear-tester. Twenty resistors were tested from each sample type. Metallographic cross-sections were also prepared from the solder joints to evaluate their microstructure. In some cases, surface cuts were prepared by a Thermo Scientific Scios 2 Focused Ion Beam (FIB) on the cross-

sections for even more detailed microstructural analysis. The microstructural and elemental investigations were done by a Thermo Scientific Scios 2 ultra-high resolution non-immersion field emission Scanning Electron Microscopes (SEM) and Energy-Dispersive X-ray spectroscopy (EDX).

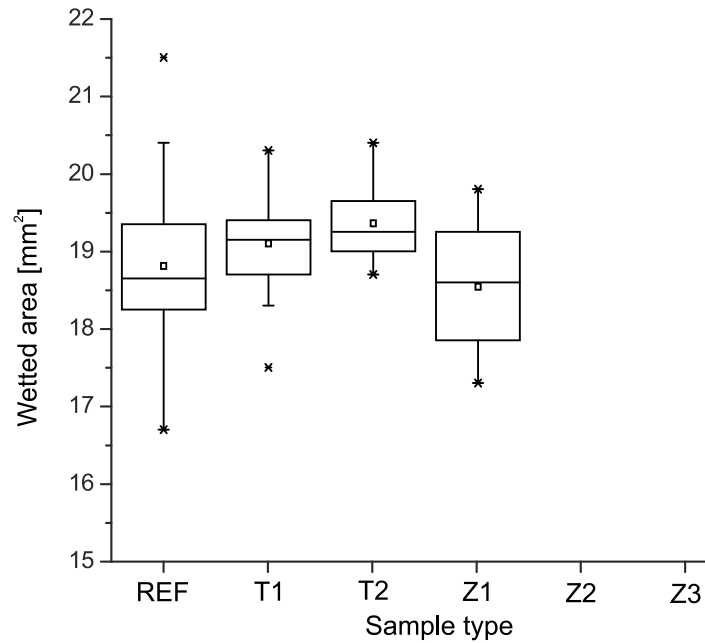
### III. RESULTS AND DISCUSSIONS

The wetting property of the nano-composite solder alloys depended on the size and the material of the added ceramics. Fig. 2 presents some examples of the spreading tests. The appearance of  $\text{TiO}_2$  nano-particles did not change the wetting properties of the nano-composite solder pastes considerably (Fig. 2b-c) compared to the reference SACX0307 (Fig. 2a). The spread areas were always continuous, and their diameters were very close to each other. In the case of the  $\text{ZnO}$  nano-particles addition (Fig. 2d-f)), the wetting behaviour of the nano-composite solder pastes decreased considerably compared to the reference SACX0307. After the addition of  $\text{ZnO}$  nano-particles having 50 and 100nm primary particle sizes (Z2 and Z3), the wetting was totally improper; the solder deposits could not reflow into a continuous surface. Therefore, the results of these samples were not evaluated further. In the case of sample Z1 ( $\text{ZnO}$  having 200nm primary particle size), the wetting was pure but still acceptable (Fig. 2d)). However, some dewetting usually occurred since the solder deposits decreased under 5mm.

The statistics of the wetted areas were calculated and showed in box plots (Fig. 3) to be able to compare the wetting results more deeply. In the box plots, the small squares show the average, the horizontal lines mark the median, the borders of the boxes show the  $\pm\sigma$  standard deviation, and the crosses indicate the min-max values. The statistical results showed a minor grew of the average wetted area in the case of  $\text{TiO}_2$  nano-particles. In addition, the fluctuation of the results also decreased since the standard deviations were smaller. The best wetting was observed in the case of  $\text{TiO}_2$  nano-particles having a primary particle size 100nm. In the case of  $\text{ZnO}$  nano-particles having a primary particle size 200nm, the average wetted area was slightly smaller than in the case of the reference SACX0307. The results of  $\text{ZnO}$  nano-particles having primary particle sizes 50 and 100 nm (samples Z3 and Z2) could not be evaluated due to improper wetting.

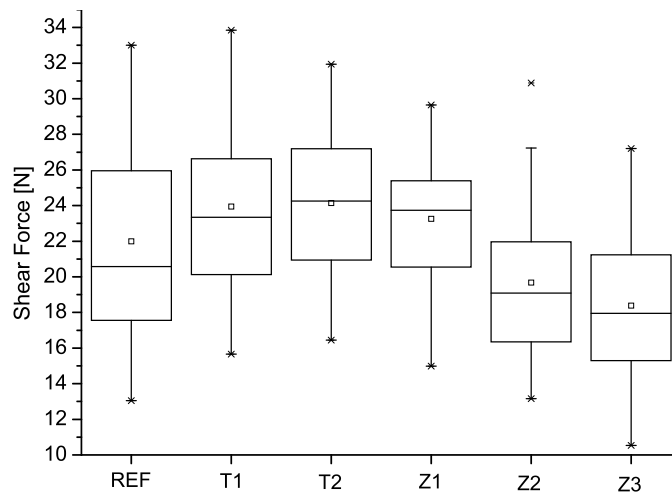


**Fig. 2.** Spreading test results.



**Fig. 3.** Statistics of the wetted areas for the different solder pastes.

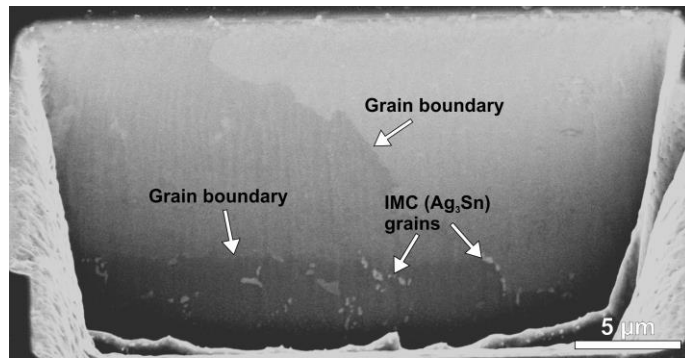
In the next step, solder joints were prepared. Fig. 4 presents the shear test results also in box plots (as it was in Fig. 3). The shear strength of the TiO<sub>2</sub> nano-composite solder joints increased compared to the simple SACX0307. The SACX0307 has an average shear strength 22N. It reached 24N in the case of TiO<sub>2</sub> nano-composites. In the case of the ZnO nano-particles the results were not obviously positive. ZnO with 200nm primary particle size (Z1) increased the average shear strength to 23N. However, in the case of Z2 and Z3 samples, a considerable shear strength drop was observed under 20N. It was caused by the improper wetting of these nano-composite solder alloys (see in Fig. 2 and 3). The best average shear strength was measured in the case of TiO<sub>2</sub> having 100nm primary particle size (T2), and it was 24N.



**Fig. 4.** Shear forces of the composite and the reference solder joints.

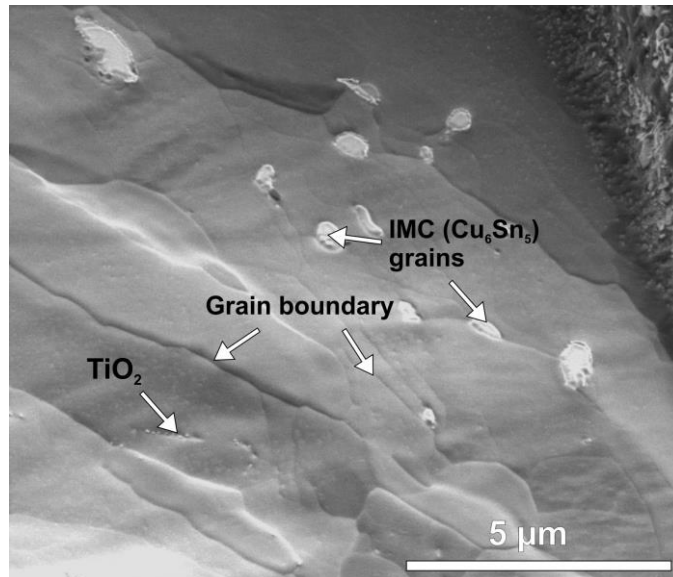
The improvement of the shear forces could not be resulted only by the slightly wetting properties of the T1 and T2 nano-composites. (Z1 samples performed even a bit weak wetting.) According to the literature [8, 17], the addition of ceramic nano-particles can refine the microstructure of solder joints. It can happen with the  $\beta$ -Sn grains and with the IMC grains as well. The refined microstructure has a better load transferability, and this results in finally the better mechanical properties of the composite solder joints. Therefore, a microstructural evaluation of the solder joints was carried out.

Fig 5. shows a SE-SEM micrograph of a FIB cut on a metallographic cross-section of a reference solder joint. Three  $\beta$ -Sn grains are visible (the grains can be distinguished by their different grayscale) with the size around 25-30  $\mu\text{m}$ . The Ag<sub>3</sub>Sn IMC grains are also visible at the grain boundary of the  $\beta$ -Sn grains.



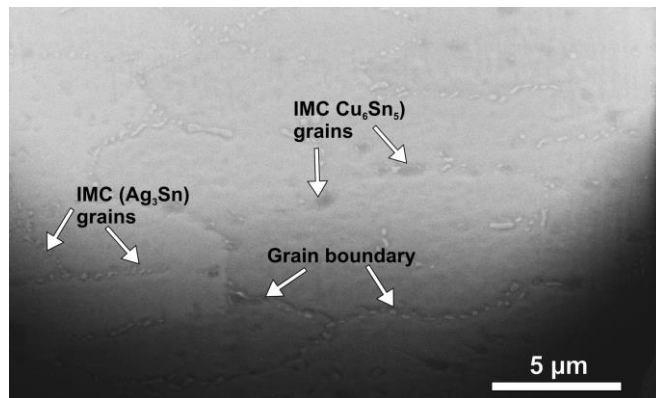
**Fig. 5.** SE-SEM micrograph of a FIB cut on the cross-section of a reference SACX0307 solder joint.

Fig 6. shows a highly magnified BSE-SEM micrograph of a FIB cut on a metallographic cross-section of a TiO<sub>2</sub> nano-composite solder joint (T2 type). It is clearly visible that considerable β-Sn grain refinement has occurred. The average grain size decreased to 3-5 μm. In this micrograph, larger Cu<sub>6</sub>Sn<sub>5</sub> IMC grains are visible at the grain boundaries of the β-Sn grains. At some parts, even the TiO<sub>2</sub> nano-particles are visible, also located at the grain boundaries of the β-Sn grains.



**Fig. 6.** BSE-SEM micrograph of the FIB cut on the cross-section of a T2 (TiO<sub>2</sub>, 100nm) nano-composite solder joint.

Fig 7. shows a BSE-SEM micrograph of a FIB cut on a metallographic cross-section of a ZnO nano-composite solder joint (Z1 type). The grain refinement of the β-Sn grains is similar as it was shown in Fig. 6. The average β-Sn grain size decreased to 5-8 μm. Here both usual IMC types (Cu<sub>6</sub>Sn<sub>5</sub> and Ag<sub>3</sub>Sn) are visible in the nano-composite solder joint.



**Fig. 7.** BSE-SEM micrograph of the FIB cut on the cross-section of a Z1 (ZnO, 200nm) nano-composite solder joint.

The microstructural investigation proved that the application of the nano-particles resulted in a considerable refinement of the  $\beta$ -Sn grains in the nano-composite solder joints. This effect could cause the improvement of the mechanical properties of the nano-composite solder joints compared to the reference SACX0307. The lower wettability of the ZnO nano-composite solder pastes could be explained that the ZnO is an amphoteric oxide, which is insoluble in water, but it can be dissolved in most acids. The base of the flux in the solder paste is acid. The chemical reaction between ZnO and acid might change the surface tension of the melted nano-composite solder alloy, and resulting in poor wetting. However, the application of highly activated fluxes could solve this problem; therefore, the ZnO nano-composite solder pastes are also promising for further application in the microelectronics industry.

#### IV. CONCLUSIONS

SACX0307-ZnO and SACX0307-TiO<sub>2</sub> nano-composite solder pastes were fabricated. The ceramic reinforcements were used in 1wt% and with different primary particle sizes between 50-200nm. The soldering properties and microstructure of the solder joints were investigated. The main conclusions are the following:

- The wetting property of the nano-composite solder alloys depended on the size and the material of the added ceramics. The TiO<sub>2</sub> nano-particles did not change the wetting properties of the nano-composite solders; however, in the case of the ZnO nano-particles, the wetting behaviour decreased considerably compared to the reference SACX0307.
- The shear strength of the TiO<sub>2</sub> nano-composite solder joints increased compared to the simple SACX0307. The results of ZnO nano-particles were not obviously positive. ZnO with 200nm primary particles size increased the shear strength; however, in the case of ZnO with smaller primary particle sizes, a considerable shear strength drop was observed
- The ceramic reinforcements caused considerable  $\beta$ -Sn grain refinement in each case. In the case of proper wetting, the considerable  $\beta$ -Sn grain refinement could cause the shear strength improvement.
- The TiO<sub>2</sub> and ZnO nano-particles are promising candidates for solder paste development; however, in the case of ZnO, more reactive fluxes are necessary to reach proper wetting.

#### V. ACKNOWLEDGEMENT

This work was partially supported by the National Research Development and Innovation Office - Hungary (NKFIH), project FK127970, and by Higher Education called "Regionalna Inicjatywa Doskonałości" in the years 2019-2022, the project number 006/RID/2018/19, the sum of financing 11 870 000 PLN".

#### REFERENCES

- [1] F. Li, V. Verdingovas, K. Dirscherl, B. Medgyes, R. Ambat, "Corrosion reliability of lead-free solder systems used in electronics", Proc. of the 2018 IMAPS Nordic Conference on Microelectronics Packaging (NordPac), 2018, pp. 67-71.
- [2] O. Krammer, T. Garami, B. Horváth, T. Hurtony, B. Medgyes, L. Jakab, "Investigating the thermomechanical properties and intermetallic layer formation of Bi micro-alloyed low-Ag content solders". J. Alloys Compd. vol. 634, 2015 pp. 156-162, 2018.
- [3] A. Skwarek, O. Krammer, T. Hurtony, P. Ptak, K. Górecki, S. Wroński, D. Straubinger, K. Witek, B. Illés, "Application of ZnO nano-particles in Sn99Ag0.3Cu0.7 based composite solder alloys", Nanomaterials, vol. 11 p. 1545, 2021.
- [4] S. Shengyan, K. Anil, Y. Jinye, W. Yanfeng, M. Haitao, W. YunpengShang, "Effect of the TiO<sub>2</sub> Nanoparticles on the Growth Behavior of Intermetallics in Sn/Cu Solder Joints", Met. Mater. Int., vol. 25, pp. 499-507, 2019.
- [5] F.C. Ani, A. Jalar, A.A. Saad, C.Y. Khor, R. Ismail, Z. Bachok, M.A. Abas, N.K. Othman, "SAC-xTiO<sub>2</sub> nano-reinforced lead-free solder joint characterizations in ultra-fine package assembly", Solde. Surf. Mount Tech., vol. 30, pp. 1-13, 2018.
- [6] Y. Tang, G.Y. Li, Y.C. Pan, "Effects of TiO<sub>2</sub> nanoparticles addition on microstructure, microhardness and tensile properties of Sn-3.0Ag-0.5Cu-xTiO<sub>2</sub> composite solder", Mater. Design, vol. 55, pp. 574-582, 2014.
- [7] C.L. Chuang, L.C. Tsao, "Effects of nanoparticles on the thermal, microstructural and mechanical properties of novel Sn3.5Ag0.5Zn composite solders", J. Mater. Sci. Mater. Electron. vol. 29, pp. 4096-4105, 2018.
- [8] AM. Yassin, H.Y. Zahran, A.F. Abd El-Rehim, "Effect of TiO<sub>2</sub> Nanoparticles Addition on the Thermal, Microstructural and Room-Temperature Creep Behavior of Sn-Zn Based Solder", J. Electron. Mater., vol 47, pp. 6984-6994, 2018.
- [9] M. Qu, T. Cao, Y. Cui, F. Liu, Z. Jiao, "Interfacial intermetallic developments of Sn-3.0Ag-0.5Cu-2.0ZnO lead free solder", J. Phy. Conf. Series, vol. 1213, pp. 1-5, 2019.
- [10] M. Qu, T. Cao, Y. Cui, F. Liu, Z. Jiao, "Effect of nano-ZnO particles on wettability, interfacial morphology and growth kinetics of Sn-3.0Ag-0.5Cu-xZnO composite solder", J. Mater. Sci. Mater. Electron., vol. 30, pp. 19214-19226, 2019.
- [11] M. Qu, T. Cao, Y. Cui, F. Liu, "Influence of ZnO nanoparticle addition on interfacial intermetallic compound evolution in Sn-3.0Ag-0.5Cu solder joints", Jap. J. App. Phy., vol. 58, pp. 1-7, 2019.
- [12] G.S. Al-Ganainy, A.A. El-Daly, A. Fawzy, N. Hussein, "Effect of adding nanometric ZnO particles on thermal, microstructure and tensile creep properties of Sn-6.5 wt%Zn-3 wt%In solder alloy", J. Mater. Sci. Mater. Electron., vol. 28, pp. 13303-13312, 2017.
- [13] A.F. Abd El-Rehim, H.Y. Zahran, A.M. Yassin, "Microstructure evolution and tensile creep behavior of Sn-0.7Cu lead-free solder reinforced with ZnO nanoparticles", J. Mater. Sci. Mater. Electron., vol 30, pp. 2213-2223, 2019.
- [14] G.S. Al-Ganainy, A.A. El-Daly, A. Fawzy, N. Hussein, "Effect of adding nanometric ZnO particles on thermal, microstructure and tensile creep properties of Sn-6.5 wt%Zn-3 wt%In solder alloy", J. Mater. Sci. Mater. Electron., vol. 28, pp. 13303-13312, 2017.
- [15] K. Kanlayasiri, N. Meesathien, "Effects of Zinc Oxide Nanoparticles on Properties of SAC0307 Lead-Free Solder Paste", Adv. Mater. Sci. Eng., Article ID 3750742, 2018.

- [16] M.A. Fatah, M. Mukhtarm, A. Abas, M.S. Haslinda, F.C. Ani, A. Jalar, A.A. Saad, M.Z. Abdullah, R. Ismail, "Effect of different S AC based nanoparticles types on the reflow soldering process of miniaturized component using discrete phase model simulation", *J. App. Fluid Mech.*, vol 12, pp. 1683–1696, 2019.
- [17] M.I.I. Ramli, N. Saud, M.A.A.M. Salleh, M.N.Derman, R.M. Said, "Effect of TiO<sub>2</sub> additions on Sn-0.7Cu-0.05Ni lead-free composite solder", *Microelectron. Reliab.*, vol. 65, pp. 255–264, 2016.